Classification of MMG Signal Based on EMD

Lulu Cheng[1], Jiejing Wang[1], Chuanjiang Li[1](✉), Xiaojie Zhan[1], Chongming Zhang[1], Ziming Qi[2], and Ziqiang Zhang[1]

[1] Mechanical and Electrical Engineering, College of Information, Shanghai Normal University, Shanghai 201418, China
Licj@shnu.edu.cn
[2] Otago Polytechnic, Dunedin, Otago, New Zealand

Abstract. Mechanomyography (MMG) signal is the sound from the surface of a muscle when the muscle is contracted. The traditional filtering algorithms for the processing of MMG signal would make most useful signal filtered when they are used to remove noise. According to MMG signal's characteristics, a new signal filtering method is presented in this paper based on combining empirical mode decomposition with digital filter, which has a better performance on MMG signal filtering processing in experimental analysis. With extracting the energy feature of wavelet packet coefficient as the feature of classifier, the BP neural network classifier gets a better classification results. The average classification results showed that the best performance for recognizing hand gestures with the energy feature of wavelet packet coefficient features was achieved by BP neural network with the accuracy of 86.41%. This work was accomplished by introducing the new signal filtering method for the recognition of different hand gestures; And suggesting basing on combining empirical mode decomposition with digital filter as a new filtering method in MG-based hand gesture classification.

Keywords: MMG · Empirical mode decomposition · Wavelet packet coefficient · BP neural network

1 Introduction

Prosthetic research focuses on the pretreatment of physiologic signal processing, classifier algorithm design, and prosthetic hand control, especially how to use the user's own signal flexibly and effectively to control an upper limb prosthesis [1, 4]. Prosthetics based on MMG signals have a very broad prospect in medical rehabilitation for the disabled, therefore its application on the medical industry is a development trend in artificial intelligence.

The vast majority of MMG signal ability focuses on the frequency range of 8–70 Hz. In this study, we investigated the potential of a multi-function muscle-interface that is controlled by MMG signals from forearm muscles.

Aiming at the characteristic of non-linear, non-stationary, and multi-forms of the MMG signal, the EMD method is used to preprocess the collected signal, and combined with the BP neural network, to research the hand gesture of classification. The EMD method is used to decompose the MMG signal containing noise, and extract

M. Fei et al. (Eds.): LSMS/ICSEE 2017, Part I, CCIS 761, pp. 23–34, 2017.
DOI: 10.1007/978-981-10-6370-1_3

the effective IMF component of the signal to reconstruction. The reconstructed signal filtered with a Chebyshev band-pass filter can obtain the effective MMG signal. Then, the effective MMG signal is decomposed by a wavelet packet to get the wavelet packet energy feature that is used as the input of the BP neural network that is established to classify the hand gesture.

2 Experiments and MMG Signal Acquisition

A convenience sample of 5 healthy individuals (4 males and 1 female), 23.5 $\pm$ 4 years of age, provide a written consent to participate in the study.

In this study, signals in the X, Y, and Z axes are detected with two three-axis Motion Tracker. A custom terminal box is built to amplify the accelerometer signals and interface the accelerometers with a terminal block. Vibrations of known amplitude are applied to each accelerometer-amplifier assembly via a mechanical shake to ensure uniform gain across all MMG sensors.

Participants sit on a chair fitted with a custom arm-rest and keep body's static state as far as possible. Two MMG sensors, manufactured according to the method of Silva J. et al. [2], are affixed to the participants' dominant forearm over extrinsic hand muscles. The two typical muscles, monitored by the sensors, are the extensor carpi radialis longus and extensor digitorum communis. Each sensor is individually affixed with a small Velcro strap.

A professional collecting software is used to start data acquisition and visually cue the participants to perform the following eight hand motions: natural state (Motion 1); hand open (Motion 2); hand close (Motion 3); wrist flexion (Motion 4); wrist extension (Motion 5); gesture "Two" (Motion 6); gesture "Five" (Motion 7); and gesture "Eight" (Motion 8). The 8 different motions are as shown Fig. 1:

Fig. 1. The eight different motion modes

The acceleration signals generated at the two muscle sites from the terminal block channeled through an analog signal conditioning input module, sampled at a rate of 200 Hz, and the digitized signals were stored on the controller's hard drive. Participants perform 80 repetitions of each of the eight motions in a pre-defined order. This process execute 200 times in total. Each motion is comprised of the full range of motion from the resting position to the target position, followed by 5 s of the hand being held in the target position. Two typical arm positions(extensor carpi radialis longus and extensor digitorum communis) commonly use in daily life activities are considered in this study for evaluating the possible effects of arm position variation on motion classification performance, which is shown on Fig. 2.

Fig. 2. Tracking sensor placement in the experiment

The three-axis Motion Tracker could collect availably three signals containing the calibrated data output of the accelerations, rate of turn and magnetic field in X, Y and Z axes. The data of the Z axis contains a majority of the effective MMG data and the other two directions' data should be thrown out. The original acceleration signal of the motion 1 collected at the extensor carpi radialis longus is shown Fig. 3.

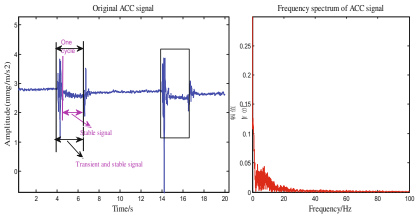

Fig. 3. Typical original signal from a forearm muscle

The acceleration signal in Z axes contains many interfering signals. In order to extract the effective MMG signal, the acceleration signals in Z axes must be made a pre-processing as shown in the following paragraphs.

3 Data Filtering Pre-processing

This paper filters the noisy signal with the Chebyshev digital filter with the method of empirical mode decomposition (EMD) combined. The Chebyshev digital filter mainly filters the direct current signal. The EMD method is used to remove the overlapping interference signals.

IMF is an intermediate product of EMD, a pre-processing algorithm of Hilbert–Huang transforms (HHTs). There are two steps involved in HHT. The first step involves the EMD to extract IMF. The second step is the Hilbert transform of the decomposed IMF to obtain a time-frequency distribution.

The EMD decomposes any signal, into a set of IMFs, each of which has a distinct time scale. It results that $x(t)$ is expressed in formula (1), as follows:

$$x(t) = \sum_{j=1}^{C} IMF_j(t) + r_C(t) \tag{1}$$

Every IMF component all are stationary signal, and directly perform Hilbert transform. The Hilbert transformation form is expressed in formula (2) as follows:

$$\overline{c_i}(t) = H[c_i(t)] = \frac{1}{\pi}\int_{-\infty}^{+\infty} \frac{c_i(\tau)}{t-\tau} d\tau, (i = 1, \ldots, n) \tag{2}$$

$c_i(t)$ and $\overline{c_i}(t)$ can constitute a complex signal $z_i(t)$ in formula (3) as follows:

$$z_i(t) = c_i(t) + j\overline{c_i}(t) = a_i(\mathrm{t})e^{y_i(t)}, (i = 1, \ldots, n) \tag{3}$$

It can get instantaneous envelope $a_i(t)$, instantaneous phase $\theta_i(t)$ and instant frequency $\omega_i(t)$ in formulas (4), (5) and (6) as follows:

$$a_i(t) = \sqrt{c_i(t)^2 + \overline{c_i}(t)^2}\,(i = 1 \cdots \cdots n) \tag{4}$$

$$\theta_i(t) = arctan\left\{\frac{Im[z_i(t)]}{Re[z_i(t)]}\right\} = arctan\left\{\frac{C_i(t)}{\overline{C}_l(t)}\right\} \tag{5}$$

$$\omega_i(t) = \frac{d\theta_i(t)}{dt} = \frac{\overline{C_I'}(t) * C_i(t) - C_i'(t) * \overline{C}_l(t)}{C_i(t)^2 + \overline{C}_l(t)^2} \tag{6}$$

Where $i = 1, \ldots, n$.

The low IMF scales mainly are the high-frequency components of signal, while the high IMF scales are the low-frequency components of signal. Thus, an EMD-based band-pass filter is developed to be use of the partial reconstruction of the selected IMF scale, which is given in formula (7) as follows:

$$EMD_K = \sum\nolimits_{i=k}^{n+1} IMF_j(t) \tag{7}$$

The effective MMG signal is decomposed to ten IMFs and every IMF is shown in the Figs. 4, 5, 6 and 7:

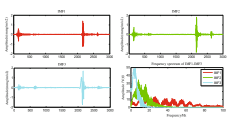

Fig. 4. The signal and frequency spectrum of IMF1- IMF3

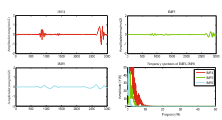

Fig. 5. The signal and frequency spectrum of IMF1- IMF3

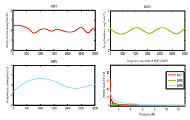

Fig. 6. The signal and frequency spectrum of IMF7- IMF9

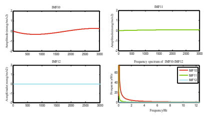

Fig. 7. The signal and frequency spectrum of IMF10- IMF12

The EMD method as a filter is essentially a partial reconstruction process of relevant modes. These modes are selected based on a given criterion that identifies the modes carrying information relevant to the main structures of the input signal [10–12].

In this paper, firstly, the EMD method is selected to filter the some interference signal overlapping the effective MMG signal in frequency spectrum. Each group data from every Tracking sensor can be decomposed to eleven IMFs. Compared with the frequency spectrum of different IFMs and the frequency band of effective MMG signal, the IMF1-IMF7 and IMF9 are selected to reconstruct the filtered signal that can represent major information of the effective MMG signal, which is mainly to solve an open question about frequency aliasing.

Then, the Chebyshev band-pass filter of Matlab library is used for filtering the low and high frequency noise. According to the effective frequency range of MMG signal, the “stop band cutoff frequency” is settled at 1 Hz to 85 Hz. Combined with Silva Jand Natasha Alves’s research [2, 3], this paper sets that the “bandpass cutoff frequency” range from 8 Hz to 70 Hz. The “minimum stop band reduction” equal to 40 dB and the “maximum passband reduction” equal to 1 dB.

Compared with the Figs. 8 and 9, it could be obviously obtain that the EMD filter makes the low frequency signal significant reduction in the amplitude of 8 Hz and the signal of other frequency also reduce a bit. The low frequency interference signal is not filtered by the classic digital filter and only filtered by the EMD method.

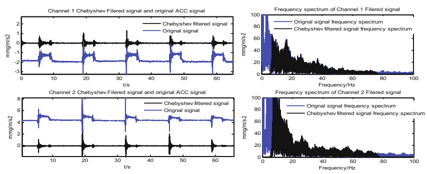

Fig. 8. Two channel MMG signal filtering using Chebyshev digital filter

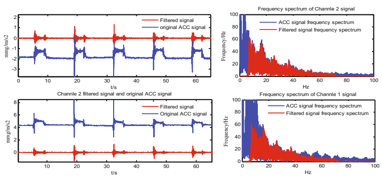

Fig. 9. Two channel MMG signal filtering using the EMD combined with Chebyshev digital filter

Although the EMD method filter remove small effective MMG signal, the feature of different motion's MMG signal becomes more obvious and it has a propitious result to classification

4 Feature Extraction

Feature extraction plays a vital role in any hand gesture recognition system based on accelerometer. Instead of dividing only the approximation spaces, wavelet packet bases present both approximation and detail spaces in a binary tree by recursive splitting of vector spaces. Any node of a binary tree is labeled by its depth j and number p of nodes (packets). Each node (j, p) corresponds to a space $W_{\mathrm{j}}^{\mathrm{p}}$, which admits an orthonormal basis $\Psi_j^p(n-2t)_{n \in Z}$. The two wavelet packet orthogonal bases at the children nodes are defined by the recursive relations in formulas (8) and (9) as follows

$$\varphi_j^{2p-1}(t) = \sum_{n=-\infty}^{\infty} h[n] \varphi_{j-1}^p(n-2t) \tag{8}$$

$$\varphi_j^{2p}(t) = \sum_{n=-\infty}^{\infty} g[n] \varphi_{j-1}^p(n-2t) \tag{9}$$

Two orthogonal spaces $W_{\mathrm{j}}^{2\mathrm{p}}$ and $W_{\mathrm{j}}^{2\mathrm{p}-1}$ can be defined as closure spaces of time-varying signals $x_{\mathrm{j}}^{2\mathrm{p}}(k)$ and $x_{\mathrm{j}}^{2\mathrm{p}-1}(k)$ respectively. Meanwhile, they can also be represented as:

$$W_{\mathrm{j}}^{\mathrm{p}} = W_{\mathrm{j}}^{2\mathrm{p}} \oplus W_{\mathrm{j}}^{2\mathrm{p}-1} \tag{10}$$

This recursive splitting defines a binary tree of wavelet packet spaces where each parent node is divided into two orthogonal subspaces. When the domain signal $\mathrm{x}(t)$ satisfies two-scale relations in formulas (11) and (12) as follows:

$$x_{j+1}^{2p}(t) = \sqrt{2} \sum h(n) x_{j+1}^{2p}(2t-n) \tag{11}$$

$$x_{j+1}^{2p}(t) = \sqrt{2}\sum g(n)x_{j+1}^{2p}(2t-n) \tag{12}$$

The expanding coefficients $h[n]$ and $g[n]$ can be expressed in the frequency domain as in formula (13) as follows:

$$H\{\cdot\} = \sum_{n=-\infty}^{\infty} h(n-2r), G\{\cdot\} = \sum_{n=-\infty}^{\infty} g(n-2r) \tag{13}$$

Let $x_{\mathrm{j}}^{\mathrm{p}}(k)$ be the pth packet on the j^{th} resolution; hence, the wavelet packet transform can be computed by the following recursive algorithm as in formulas (14), (15), (16) and (17) as follows:

$$x_0^1(k) = x(t) \tag{14}$$

$$x_j^{2p-1}(k) = Hx_{j-1}^p(k) \tag{15}$$

$$x_j^{2p}(k) = Gx_{j-1}^p(k) \tag{16}$$

$$x_j^p(k) = x_j^{2p-1}(k) + x_j^{2p}(k) \tag{17}$$

Where $k = 1, 2, \ldots, 2^{J-P}, P = 1, 2, \ldots, J$ and $J = log_2 N$.

The paper uses 6^{th} wavelet packet to decompose the effective MMG signal and each one senor signal can get twenty-five wavelet trees with different frequency. The order of wavelet packet is determined by empirical value. The 6 order is optimal result and it is determined with a mount of experiments using different order of wavelet packet to extract features to test the classification accuracy. Wavelet coefficient energy can be counted by extracting the coefficients of the wavelet packet frequency bands. S_{6j} represents the fifth layer wavelet of the j^{th} node of packet signal $x_i^j(k)$ coefficient. The j^{th} node of wavelet coefficient energy can be represented as in formula (18) as follows:

$$E_N^j = \sum\nolimits_{i=1}^{N-1} \left(S_{6j}\right)^2, (i = 0, 1, \ldots, N-1) \tag{18}$$

Where N represents the wavelet packet decomposition layer, j represents the nodes of the wavelet packet.

The feature vector M that it is determined by the BP neural network structure as follows in formula (19), which is consisted of the vector E_{ab}^j. The vector E is consisted of the all 25 nodes of the wavelet packet energy value of two Tracking sensors, is as follows in formula (20):

$$E_{ab}^j = \left[E_{11}^0, \ldots, E_{11}^{24}, E_{21}^0, \ldots, E_{21}^{24}\right] \tag{19}$$

$$M_{bn} = [E_{11}E_{12}\ldots E_{1n}E_{21}\ldots E_{2n}\ldots E_{81}E_{82}\ldots E_{8n}] \tag{20}$$

Where $a = 1, 2$, represent Tracking sensor's number, $b = 1, 2, 3, \ldots 8$, represent the type of gesture movement, n represent the number of sample.

5 Classifier Processing

BP neural network is essentially a sample set of the input and output that is transformed into a nonlinear optimization problem. It is a learning algorithm through the gradient algorithm to solve the question of the weight.

This paper adopts standard three-layer BP neural network and uses self-adapting gradient descent algorithm to improve network performance with the optimal parameters for the best recognition rate for Finger motion. The standard three-layer BP neural network model is shown in Fig. 10:

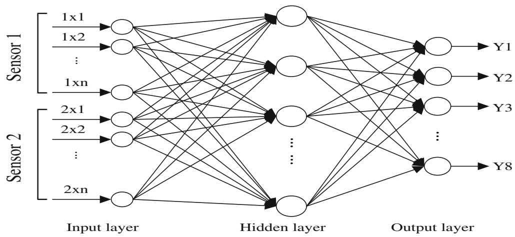

Fig. 10. BP neural network structure mode

The hidden layer node: The number of neurons in the hidden layer is usually more than the number of the input factors and hidden layer neurons of 7–15 are appropriate, so the number of hidden neurons is 12.

Output layer node: BP neural network number of hand gesture is the number of output neurons, so the output layer of the network of each neuron corresponds to a class. The eight motion modes respectively corresponding to the target output vector. According to the above method, the node number is: 50, 12 and 8.

Learning rate: the value is 0.08 according to many experimental results.

6 Pattern Recognition Analysis and Results

In this chapter, the experiment selects the first 100 groups of data to train the sample to acquire the proper weights and thresholds and the remaining 100 groups' data to test the classification accuracy of the finger motion.

In the experiment, the two groups' data pass pretreatment, and are extracted the training feature sets and test feature sets. Then, BP neural network is used to train characteristics training set and sets the maximum training accuracy of the training network at 10^{-4}. BP neural network achieves the expected accuracy requirements after 8000 iterations training.

In the study, experiment will use two methods to confirm the effectiveness of finger motion's recognition, which is different filter method for the purpose of individual-validation and cross-validation. Detailed experimental procedure is described below.

Firstly, in the experiment, the two groups' data pass Chebyshev filter, and the features of wavelet packet coefficient energy separately are extracted to form the training set and test set. Then, the training sets are imported to train the three layers of BP neural network and the optimal parameter matrix is acquired. The average false recognition rate of each group of samples and the false recognition rate of each action was calculated. The results are shown in Fig. 11:

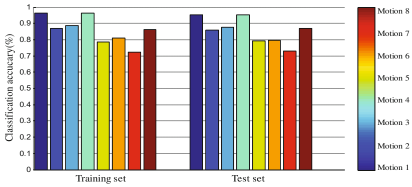

Fig. 11. The classification recognition accuracy of hand gestures with the Chebyshev digital filter.

Secondly, the two groups' data pass the Chebyshev band-pass filter combined with the EMD method, and the features of wavelet packet coefficient energy separately are extracted to form the training set and test set. Figure 12 shows the recognition precision of hand gesture recognition.

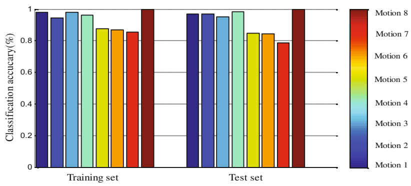

Fig. 12. The classification recognition accuracy of hand gestures with the EMD filtering method combined with Chebyshev digital filter

Finally, we use the cross-validating method to validate the advantage of EMD method in the hand gesture recognition. In this paper, cross-validating method is used for testing the classification accuracy. This method is explained that the prostheses is only designed for special disabled, so the validation sets must come from entirely same subjects in consideration to the prostheses characteristic. Research should be sure that the result of classification accuracy is not influenced by the collecting order of training sets. In order to avoid the over-fitting of BP neural network, the remaining 100 groups' data randomly is divided into five groups. then, among four groups' data are used for training set and the remaining one group data is used for test set until the every group

Table 1. The recognition accuracy of hand gestures cross-validation method.

Example	Subject 1	Subject 2	Subject 3	Subject 4	Subject 5
Test 1	87.78%	86.89%	89.07%	85.75%	82.29%
Test 2	89.03%	88.21%	90.64%	86.06%	81.77%
Test 3	88.69%	89.42%	88.88%	88.30%	79.84%
Test 4	86.34%	87.09%	90.05%	86.66%	81.63%
Test 5	90.01%	89.44%	86.39%	87.69%	82.76%
Average	88.31%	87.08%	88.74%	86.34%	81.52%

data all is used for test set. The average recognition rate of 5 times examples are counted and the results is shown in the Table 1 (The Subject 1, Subject 2, Subject 3 and Subject 4 is male with strong body and muscle and the subject 5 is a health female. The result in Table 1 is the average classification.):

The Table 1 can get the conclusion that the difference of muscle leads to that the MMG signals collected by Motion Tracker have apparent difference, which directly influence the classification accuracy. The recognition accuracy of cross-validating is close to the recognition accuracy of test set using the EMD method.

The experiment results show that the maximum error of eight kinds of gesture recognition using BP neural network algorithm for EMD signal is about 13.59%, and the average accuracy of eight kinds of gesture motion pattern recognition rate is 86.41% in the condition of individual-validation. But the accuracy of the cross-validation decreases in a degree, because the different subject's muscle is different and leads to that the MMG signal collected has a bit diversity.

7 Conclusion

In the analyzing of the MMG signal with non-stationary and nonlinear characteristic, this study uses the method of combining the EMD with the classical digital filter to remove the noise and the better results are obtained. Compared with the traditional time domain and frequency domain analysis method, the EMD combined with the band pass filter can effectively filter out the noise signal that is same with the MMG signal frequency spectrum. The study show that this method can effectively identify the pattern classification of eight kinds of action and the average recognition rate reached 86.41% using 50 features.

Compared with Natasha Alves's mean accuracy of $93 \pm 0.9\%$ using 15 features for eight classes of forearm muscle activity using LDA in 2009 and 2010 [1], Yanjuan Geng's the average 90% classification error with two-channel ACC-MMG signals about sevsen classes of forearm muscle activity using LDA in 2012 [4] and Lou'I Al-Shrouf's 75% accuracy to classify five hand-motions with five ACC sensors using STFT-SVM in 2014 [6], a certain practical value can be shown in this study, which only use two-channel ACC-MMG signals to classify eight forearm muscle activities.

Acknowledgments. 1. Supported by research project of Science and Technology Commission of Shanghai Municipality (Project Number: 16070502900) 2. Supported by the Program of Shanghai Normal University (A-7001-15-001005)

References

1. Alves, N., Chau, T.: Classification of the mechanomyogram its potential as a multifunction access pathway. In: Annual International Conference of the IEEE Engineering in Medicine and Biology Society, pp. 2951–2954 (2009)
2. Silva, J., Heim, W., Chau, T.: MMG-based classification of muscle activity for prosthesis control. In: Proceeding of IEEE Conference on Engineering Medical Biology Society science, vol. 2, pp. 968–971 (2004)
3. Alves, N., Sejdi, E., Sahota, B., Chau, T.: The effect of accelerometer location on the classification of single-site forearm mechanomyograms. BioMed. Eng. Online **9**(1), 1–14 (2010)
4. Geng, Y., Zhou, P., Li, G.: Toward attenuating the impact of arm positions on electromyography pattern-recognition based motion classification in trans radial amputees. J Neuro. Eng. Rehabil. **9**, 74 (2012)
5. Khan, A.M., Siddiqi, M.H., Lee, S.-W.: Exploratory data analysis of acceleration signals to select light-weight and accurate features for real-time activity recognit ion on smartphones. Sensors **13**(10), 13099–13122 (2013)
6. Al-Shrouf, L., Saadawia, M.S., Söffker, D.: Improved process monitoring and supervision based on a reliable multi-stage feature-based pattern recognition technique. Inf. Sci. **259**, 282–294 (2014)
7. Daoud, H.-G., Ragai, H.-F.: Mechanomyogram signal detection and decomposition. conceptualisation and research. Int. J. Healthcare Technol. Manag. **13**(1–3), 32–44 (2012)
8. Xie, H.-B., Zheng, Y.-P., Guo, J.-Y.: Classification of the mechanomyogram signal using a wavelet packet transform and singular value decomposition for multifunction prosthesis control. Physiol. Meas. **30**(5), 441–457 (2009)
9. Chang, K.-M., Liu, S.-H.: Gaussian noise filtering from ECG by wiener filter and ensemble empirical mode decomposition. J. Signal Process. Syst. **64**(2), 249–264 (2011)
10. Komaty, A., Boudraa, A.-O., Augier, B., Dare-Emzivat, D.: EMD-based filtering using similarity measure between probability density functions of IMFs. Instrum. Meas. IEEE Trans. **63**(1), 27–34 (2014)
11. Yang, Z., Yu, Z., Xie, C., Huang, Y.: Application of Hilbert-Huang transform to acoustic emission signal for burn feature extraction in surface grinding process. Measurement **47**, 14–21 (2014)
12. Guo, K., Zhang, X., Li, H., Meng, G.: Application of EMD method to friction signal processing. Mech. Syst. Signal Process. **22**(1), 248–259 (2008)
13. Li, M., Wu, X., Liu, X.: An improved emd method for time–frequency feature extraction of telemetry vibration signal based on multi-scale median filtering. Circuits Syst. Signal Process. **34**(3), 815–830 (2015)
14. Rilling, G., Flandrin, P., Goncalves, P.: On empirical mode decomposition and its algorithms. In: IEEE - EURASIP Workshop on Nonlinear Signal and Image Processing. Grado(I), pp. 8– 11 (2003)

15. Liu, Y., Li, Y., Lin, H., Ma, H.: An amplitude-preserved time-frequency peak filtering based on empirical mode decomposition for seismic random noise reduction. Geosci. Remote Sens. Lett. IEEE **11**(5), 896–900 (2014)
16. Chatlani, N., Soraghan, J.J.: EMD-Based Filtering (EMDF) of low-frequency noise for speech enhancement. IEEE Trans. Audio Speech Lang. Process. **20**(4), 1158–1166 (2012)